



HAL
open science

A reduced model of cell metabolism to revisit the glycolysis-OXPHOS relationship in the deregulated tumor microenvironment

Pierre Jacquet, Angélique Stéphanou

► **To cite this version:**

Pierre Jacquet, Angélique Stéphanou. A reduced model of cell metabolism to revisit the glycolysis-OXPHOS relationship in the deregulated tumor microenvironment. *Journal of Theoretical Biology*, 2023, 562, pp.111434. 10.1016/j.jtbi.2023.111434 . hal-03973607

HAL Id: hal-03973607

<https://hal.science/hal-03973607>

Submitted on 4 Feb 2023

HAL is a multi-disciplinary open access archive for the deposit and dissemination of scientific research documents, whether they are published or not. The documents may come from teaching and research institutions in France or abroad, or from public or private research centers.

L'archive ouverte pluridisciplinaire **HAL**, est destinée au dépôt et à la diffusion de documents scientifiques de niveau recherche, publiés ou non, émanant des établissements d'enseignement et de recherche français ou étrangers, des laboratoires publics ou privés.

A reduced model of cell metabolism to revisit the glycolysis-OXPHOS relationship in the deregulated tumor microenvironment

Pierre Jacquet and Angélique Stéphanou*

Université Grenoble Alpes, CNRS, TIMC-IMAG/DyCTIM2, 38041 Grenoble, France

February 4, 2023

* Corresponding author's E-mail: angelique.stephanou@univ-grenoble-alpes.fr

Abstract

Cancer cells metabolism focuses the interest of the cancer research community. Although this process is intensely studied experimentally, there are very few theoretical models that address this issue. One of the main reasons is the extraordinary complexity of the metabolism that involves numerous interdependent regulatory networks which makes the computational recreation of this complexity illusory. In this study we propose a reduced model of the metabolism which focuses on the interrelation of the three main energy metabolites which are oxygen, glucose and lactate in order to better understand the dynamics of the core system of the glycolysis-OXPHOS relationship. So simple as it is, the model highlights the main rules allowing the cell to dynamically adapt its metabolism to its changing environment. It also makes it possible to address this impact at the tissue scale. The simulations carried out in a spheroid show non-trivial spatial heterogeneity of energy metabolism. It further suggests that the metabolic features that are commonly attributed to cancer cells are not necessarily due to an intrinsic abnormality of the cells. They can emerge spontaneously due to the deregulated over-acidic environment.

Keywords: acidity; theoretical model; energetic needs; pyruvate-lactate; Warburg effect

1 Introduction

The energy metabolism of cancer cells has been the subject of extensive research for over fifty years, yet the mechanisms governing tumor metabolism are not clearly understood. The Warburg effect, which now appears to be accepted as a key feature of many types of cancer, is considered by some as one possible fundamental cause of cancer [1, 2]. Some define this effect as a high lactate production despite a sufficient oxygen supply [1, 3]. However according to Warburg's original observations in the 1920s, the effect is limited to the tumor producing a large amount of lactate (regardless of the presence of oxygen) [4–6]. This lactate production is induced by high glycolytic activity and increased glucose uptake. This creates around the cells, and in particular within solid tumors, a whole microenvironment, characterized by an acidic pH, favoring the invasion of tumor cells. A recurring question remains "how do these extreme conditions benefit the cell?" [7–9]. Understanding the impact of the microenvironment on ATP production may be part of the answer.

The purpose of this paper is to address this issue with a reduced mathematical model of cell metabolism limited to the glycolysis-OXPHOS relationship to highlight the consequences on this duo and provide a new understanding of cell energy metabolism.

Cell metabolism is highly complex because it is a multifactorial mechanisms that involves many different interacting processes with many different actors. Moreover it is an evolving process and although crucial, this aspect is rarely considered and often overlooked. In this context, a theoretical model is a powerful and efficient way to make sense of this complexity and to address temporality. It makes it possible to test the relevance of new hypotheses and to exhibit emergent properties that cannot be intuited, in order to better understand the intimate functioning of metabolic processes and also to provide new insights to guide future research.

Several models have been proposed to describe cell energy metabolism [10–14] but some may be too complex to be easily reused and tested by experimentation. We therefore focused more specifically on models describing the production of ATP as a function of the conditions surrounding the cell. Extracellular oxygen and glucose concentrations, lactate production and the quantification of extracellular pH (by protons secretion) are the conditions that were mainly taken into account in the modeling. The availability of glucose and oxygen influences the activity of glycolysis and oxydative phosphorylation (OXPHOS), respectively. Casciari *et al.*, (1992) [15, 16] proposed a model which describes changes in glucose and oxygen consumption in EMT6/Ro cells. They raised the importance of pH on these uptakes and mathematically formalized these observations. This pioneering model – which exploits experimental data – has since been used in several studies [11, 17, 18].

Our computational model is again primarily based on this reference model. However, it additionally integrates the most recent knowledge, in particular the disappearance of the Warburg phenotype under acidic conditions [19], and is rooted on new key observations and established facts. The model once again focuses on the glycolysis-OXPHOS relationship but emphasizes the role of lactate as a substrate. Lactate is indeed of particular interest because it can allow tumor cells to survive despite a significant depletion of glucose [20]. Its role for cell viability under acidic conditions has been overlooked since very few models integrate this important fact.

Our model also takes into account the central role of pyruvate in the regulation of the metabolism. It may seem trivial to recall that, glycolysis is the set of reactions that transform glucose into pyruvate, but

sometimes glycolysis is mentioned as the complete transformation of glucose into lactate (also called fermentation). This is a source of misunderstanding, as it suggests that glycolysis opposes the mitochondrial metabolic pathway that would be an independent process. In fact the Krebs cycle and the OXPHOS which results from it, require pyruvate resulting from glycolysis under normal conditions, as a first step, hence its pivotal role. These paths, although running in parallel in the cell, are in reality a chain of reactions and not dual options which exclude one another.

The model then investigates how imposed environmental constraints and the imposed energy needs of the cell push the cell to adapt its metabolism to meet its needs. The simulations performed are insightful since they clearly show how glycolysis and OXPHOS are used concomitantly and cooperatively [21]. The gradation in their relative contributions to ATP production has been shown to depend on available resources and environmental acidity.

2 Materials and Methods

2.1 Modeling approach and model assumptions

Our modeling approach is oriented towards a global understanding of an idealized aspect of cell metabolism. Cell metabolism is highly complex and exhibits a wide diversity of responses among cells. All cells do not behave in the same way under the same environmental constraints. However, there are some fundamental principles that have yet to be elucidated. The aim of our model is to focus on the relationship between OXPHOS and glycolysis where we specifically look at the impact of acidity on this relationship and the role that pyruvate can play as a regulatory agent in the absence of other regulation. This implies using a reduced model which only retains the main players in this relationship, which means that the many other regulatory processes of the enormous metabolic machinery are not taken into account. The system we are studying is therefore only a subsystem of this global machinery, studied in isolation to exhibit its fundamental principles.

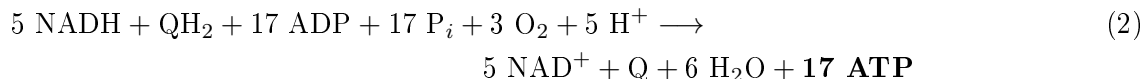
We focus on the glycolysis-OXPHOS system, as well as the place of lactate within it. It is nevertheless important to remember that other pathways such as β -oxidation of fatty acids or glutaminolysis can contribute to increasing the reaction intermediates and thus increase the energy production capacity.

In order to define our model, we first recall some fundamental concepts of the metabolism of these two pathways. Glucose is considered as the main source of energy for the cell. This molecule is catabolized during a sequence of three processes essential to produce ATP. The first reaction, glycolysis, transforms glucose into pyruvate as follows:



NAD^+ is rate limiting for glycolysis, in the reaction catalyzed by Glyceraldehyde 3-phosphate dehydrogenase (GAPDH). But in the overall fermentation / respiration process, the NAD^+ pool is refilled by LDH, or oxydative phosphorylation. If the ratio $\text{NAD}^+ / \text{NADH}$ is too low, glycolysis will be inhibited. Numerous metabolic reactions modify this ratio and more generally the redox state of the cell. Here the goal is not to model all the mechanisms which can lead to changing the $\text{NAD}^+ / \text{NADH}$ ratio. We therefore consider that NAD^+ is not limiting for the processes we seek to observe.

Pyruvate can be reduced to lactate with lactate dehydrogenase (LDH) but the reaction will not produce more ATP. Pyruvate can also be decarboxylated by the pyruvate dehydrogenase in Acetyl-CoA. This decarboxylation takes place in the mitochondria. If the pyruvate is converted into lactate, the latter, under physiological conditions, will be secreted in the extracellular space by MCT transporters. Otherwise, the pyruvate is converted to Acetyl-CoA, which enters the citric acid cycle, generates one GTP (equivalent to one ATP) and generates NADH and coenzyme Q, QH₂ used in the final step of the reaction. It is the OXPHOS, in which the energy released by the transfer of electrons from a donor to an acceptor (notably oxygen), which is used to produce a large amount of ATP (from ADP). This final reaction can be summarized as follows:



Each reaction is written in its canonical form. From one glucose molecule, the cell can obtain a total of 38 ATP molecules. Currently, the estimation of the number of ATP molecules produced during aerobic respiration is still under debate (38 is a theoretical maximum) [22, 23]. We will continue our calculation with 17 moles of ATP per mole of pyruvate [17]. It is also relevant to note that in several experiments the level of pyruvate remains relatively constant (regardless of the microenvironment) [19]. We therefore hypothesize that pyruvate functions as a reservoir that flows according to the mitochondrial energy needs. If this reservoir overflows (too much pyruvate produced), the excess is converted into lactate. Conversely, if it empties faster than it fills (not enough pyruvate), production or consumption can be readjusted (by reabsorbing lactate for example). We note that the PKM2 (Pyruvate Kinase) enzyme is limiting in the final reaction of pyruvate production. This enzyme is tightly regulated and this regulation determines whether glycolytic intermediates before pyruvate should be used in synthesis of amino-acid/nucleic acid or not. In a cancer scenario, the PKM2 enzyme is mainly in its inactive dimeric form but can switch to its trimeric form by the accumulation of Fructose 1,6-bisphosphate (FBP) which leads to the conversion of most glycolytic intermediates to pyruvate [24]. The tetramer/dimer ratio of PKM2 enzyme oscillates [25]. This mechanism is not studied here but could modify the temporal dynamic of glycolysis. However, the fact that a large amount of lactate is produced in cancer cells, indicates that over a longer period of time, the PKM2 enzyme still allows the reaction to take place. Pyruvate can also be produced from oxaloacetate by pyruvate carboxylase to remove excess oxaloacetate in the TCA cycle. Finally pyruvate is also used to produce alanine. These two mechanisms are not considered in this model.

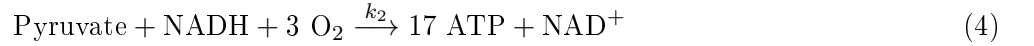
The model is based on the following experimental observations:

1. Glucose consumption increases with glucose concentration, oxygen consumption increases with oxygen concentration [15, 26] and lactate consumption increases with lactic acidosis [19, 27], meaning that the substrates directly influence consumption rates.
2. The less oxygen there is in the extracellular medium, the more glucose consumption increases [28] up to a saturation threshold [15]. Indeed, if one pathway of ATP production slows down, the other takes over to guarantee steady-state ATP levels and this requires an increase in the corresponding uptakes.
3. The more acidic the medium (the protons concentration is high), the lower the glycolysis. Acidification of the medium slightly lowers the intracellular pH, and decreases the activity of glycolytic enzymes. This causes an increase in intracellular glucose, which at one point leads to a decrease in glucose uptake [15, 19, 29, 30].

4. The pyruvate concentration remains relatively constant [19]. The maintenance of this constant level is mainly enabled by several mechanisms: the regulation of its production by glycolysis, the regulation of its consumption in respiration, its excretion by lactate and its regeneration from lactate.

2.2 Model equations

To estimate the rate of ATP production per cell, it is necessary: (i) to evaluate the rates of cell consumption of glucose, oxygen and lactate which are three limiting substrates for energy production and (ii) to understand how these different consumption rates vary depending on the environmental conditions. ATP production comes from two main processes and can therefore be represented in two parts. The first part, is the ATP produced by glycolysis and the second one, the ATP produced by OXPHOS, if there is enough pyruvate and oxygen in the medium. As in Jagiella et al. (2016)[17], we respectively summarize these reactions under the two highly simplified forms:



Assuming that changes in glucose and oxygen concentrations in cells depend primarily on their consumption and uptake rates, they write:

$$\frac{d[G]}{dt} = \underbrace{-k_1[G]}_{\text{Glucose consumption}} + \underbrace{U_G}_{\text{Glucose uptake}} \quad (5)$$

$$\frac{d[O_2]}{dt} = \underbrace{-k_2[Pyruvate][O_2]^3}_{\text{Oxygen consumption}} + \underbrace{\frac{U_{O_2}}{3}}_{\text{Oxygen uptake}} \quad (6)$$

And, according to reactions (3) and (4), the evolution of the ATP concentration is given by the contributions of glycolysis and OXPHOS that respectively provide 2 and 17 ATP from the glucose and oxygen consumed:

$$\frac{d[\text{ATP}]}{dt} = 2k_1[G] + 17k_2[Pyruvate][O_2]^3 \quad (7)$$

where $[G]$, $[O_2]$, $[\text{ATP}]$ and $[Pyruvate]$ are the intracellular concentrations of glucose, oxygen, ATP and pyruvate respectively. k_1 is the rate of glycolysis and k_2 is the oxygen consumption rate through the citric acid cycle and OXPHOS combined. Given the equilibrium condition where the uptake of glucose and oxygen are equal to their respective consumption, *i.e.* $U_G = k_1[G]$ and $U_{O_2}/3 = k_2[Pyruvate][O_2]^3$, by identification with equation (7), we get the following equation:

$$\frac{d[\text{ATP}]}{dt} = 2U_G + \frac{17}{3}U_{O_2} \quad (8)$$

It is then necessary to evaluate respectively the glucose and oxygen consumption rates U_G and U_{O_2} . Casciari *et al.*, (1992) [15] proposed a model, based on experiments on EMT6/Ro cells, where the uptake depend on the concentrations of the substrates and on the pH. This model has been used and modified

several times to describe the growth of spheroids [17] or to estimate the amount of ATP produced [11, 18]. However, the model does not integrate the energetic role of lactate. Only the acidification of the medium is taken into account. According to *observation 3*, this implies a significant drop in glucose consumption which raises the problem of the stability of the ATP level since it cannot be maintained for long enough.

We built our model of cell metabolism considering that oxygen consumption does not directly depend on glucose concentration by contrast with other existing models [13, 15, 17, 18]. In our model (Fig 1), ATP is the factor that links oxygen consumption to glucose consumption. If enough ATP is produced this inhibits the OXPHOS, which leads to the decrease of the oxygen consumption in the first place. This new hypothesis releases a strong constraint on the system and allows more flexibility with the potential to generate more metabolic behaviors. *In vivo*, OXPHOS is not directly limited by ATP (however the reduction of ADP pool reduces its activity). But TCA enzymes like isocitrate dehydrogenase or oxoglutarate dehydrogenase are inhibited by ATP and NADH. By limiting these steps there is less NADH produced that can be used later for OXPHOS. In addition, the less oxygen there is, the more glucose consumption increases. Indeed, when the cell lacks oxygen, HIF is stabilized and upregulates the expression of glycolytic enzymes [31–33]. This improvement in the model makes things more natural (*i.e.* more emergent).

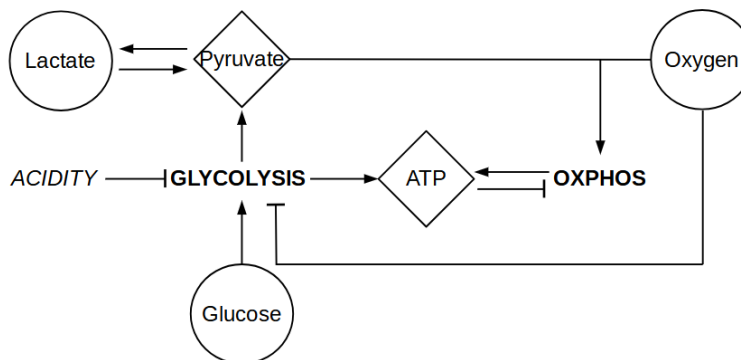


Figure 1: Overview of the model. Circular boxes represent the extracellular substrates, diamond boxes represent the intracellular proteins or molecules.

2.2.1 Glucose uptake rate, U_G

According to experimental *observation 1*, glucose uptake increases with the concentration of extracellular glucose up to a saturation threshold. The simplest way to represent this property is to use a Henri-Michaelis-Menten function:

$$U_G = V_G^{max} \times \frac{[G]}{K_G + [G]} \quad (9)$$

where K_G is the Michaelis constant for glucose consumption and V_G^{max} is the maximum uptake rate of glucose at saturation. First, the less oxygen there is, the more V_G^{max} increases (*observation 2*). In addition, the more acidic the medium, the more V_G^{max} decreases (*observation 3*). This is also true when the pH becomes alkaline [34]. V_G^{max} is therefore expressed by the combination of these two effects as follows:

$$V_G^{max} = U_G^{max} \times \left(\frac{p_G^{O_2}}{p_G^{O_2} + [O_2]} \right) \times \left(p_G^{pH_{max}} \times \exp \left(-\frac{(\text{pH} - \text{pH}_{max})^2}{2\sigma^2} \right) \right) \quad (10)$$

where U_G^{max} is the physiological uptake limit of glucose and $p_G^{O_2}$ is a constant for glucose uptake variations as a function of oxygen level. The term related to the pH has a Gaussian form, which (i) varies from close to 0, when the pH is acidic, to 1 when it is physiological (pH \approx 7.3), (ii) reaches a maximum at pH $_{max}$, which is the pH corresponding to the maximum glucose uptake and (iii) then decreases. $p_G^{pH_{max}}$ is the maximum expression of glucose uptake when the pH is optimal and σ is a constant that tunes the spread in the Gaussian term of the glucose uptake.

2.2.2 Oxygen uptake rate, U_{O_2}

As for glucose and according to *observation 1*, oxygen uptake is described with a Henri-Michaelis-Menten function:

$$U_{O_2} = V_{O_2}^{max} \times \frac{[O_2]}{K_{O_2} + [O_2]} \quad (11)$$

where K_{O_2} is the Michaelis constant for oxygen consumption and $V_{O_2}^{max}$ is the maximum uptake rate of oxygen at saturation.

Unlike glucose, the diffusion of oxygen across the plasma membrane is passive diffusion. Thus, it can be considered that the oxygen concentration at equilibrium, outside and inside the cell is almost identical. Only the oxygen consumption by the cell governs the inflow. The main role of OXPHOS is to supply the ATP needed by the cell and the rate of ATP synthesis by OXPHOS is tightly coupled to the rate of ATP utilization [35]. Rather than varying the oxygen consumption according to the glucose concentration as in previous models [11, 15, 17], we hypothesize that it varies directly according to the need for ATP not filled by glycolysis. Indeed, there is no molecular proof allowing to directly link the evolutions of the two substrates. There are, in the other hand, a multitude of other signals which indirectly link the two. If the cell needs a specific ATP level (ATP $_{target}$), the mitochondria must produce the missing part of ATP (ATP $_{target}$ - ATP $_{glycolysis}$) to complete the part produced by glycolysis (ATP $_{glycolysis}$).

From (eq.2) and (eq.8), to produce 1 mole of ATP, the mitochondria needs 3/17 mole of oxygen. For 3 moles of oxygen, one mole of pyruvate is consumed. Taking into account the fact that the pyruvate level can be limiting, $V_{O_2}^{max}$ is expressed by the following expression:

$$V_{O_2}^{max} = \min \left(3 \times [Pyr], \quad p_{O_2}^{ATP} \times \frac{3}{17} (\text{ATP}_{target} - \text{ATP}_{glycolysis}) \right) \quad (12)$$

with $p_{O_2}^{ATP}$, the rate of production for missing ATP.

2.2.3 Lactate uptake rate, U_L

Lactate can be produced and secreted as well as consumed. Again, as for glucose and oxygen, lactate uptake can be written with the following expression (*observation 1*):

$$U_L = V_L^{max} \times \frac{[L]}{K_L + [L]} \quad (13)$$

where $[L]$ is the lactate concentration and K_L is the Michaelis constant for lactate consumption. Xie *et al.*, (2014) [19], measured the amount of lactate consumed as a function of the level of lactic acidosis. They showed that in a low pH environment, the higher the extracellular lactate level, the more lactate uptake increases to the point where the inflow exceeds the outflow (*observation 4*). Lactate transport is mediated by monocarboxylate transporters (MCT), a group of plasma membrane transporters bound to protons. A proton gradient between the outside and the inside of the cell is necessary to transport the lactate [36]. The parameter V_L^{max} is therefore taken as a Hill function which decreases with increasing pH.

$$V_L^{max} = U_L^{max} \times \left(1 - \frac{\text{pH}^n}{(K_{\text{pH}})^n + \text{pH}^n} \right) \quad (14)$$

2.2.4 Pyruvate fate and Lactate secretion

The change in intracellular pyruvate concentration is written as:

$$\frac{d[\text{Pyr}]}{dt} = \underbrace{\left(2U_G \right)}_{\text{GLYCOLYSIS}} - \underbrace{\left(\frac{1}{3}U_{O_2} \right)}_{\text{OXPHOS}} + \underbrace{U_L}_{\text{Pyr} \leftarrow \text{Lac}} - \underbrace{S_L}_{\text{Lac} \leftarrow \text{Pyr}} \quad (15)$$

Xie *et al.*, (2014) [19] observed that the level of pyruvate remains constant regardless of the pH and lactate conditions (*observation 4*). In this case, the preceding formula can be written:

$$2U_G + U_L = \frac{U_{O_2}}{3} + S_L \quad (16)$$

Finally, pyruvate converted to lactate corresponds to the "excess" pyruvate, $[\text{Pyr}]_{\text{Target}}$ being the basal concentration in the cell. Since this is a surplus, this term should not be negative:

$$S_L = \min \left(0, \quad p_{\text{Lac}}^{\text{Pyr}} \times ([\text{Pyr}]_{\text{Target}} - [\text{Pyr}]) \right) \quad (17)$$

with $p_{\text{Lac}}^{\text{Pyr}}$, the rate of production for missing Pyruvate.

The functions defined in (eq.9-14) are adjusted and parameterized from experimental data. Table 1 summarizes the values used in the model and their sources.

2.3 Simulations

2.3.1 Individual cell level

To simulate the evolution of metabolic molecules, we used the *DifferentialEquations.jl* module (v 1.10.1)[38] from the Julia language (v 1.1.1). This module integrates many solvers of Ordinary Differential Equations (ODE) and we have chosen the solver *AutoTsit5-Rosenbrock23*, which allows to automatically choose the

¹This parameter is set high to accelerate the simulation (this does not change the conclusions of the simulation) the value usually observed is around: $[0.1-1] \times 10^{-16} \text{ mM.s}^{-1}$, see [15, 17].

²This parameter is also set high to match the high uptakes, the value usually observed is around: $[0.1-1] \times 10^{-15} \text{ mM.s}^{-1}$, see [17, 18]

Table 1: Parameter values used to perform the simulations

Symbol	Value	Description	References
$[G]$	[0, 15] mM	Extracellular concentration of glucose	[15]
$[O_2]$	[0, 0.1] mM	Extracellular concentration of oxygen	[15]
$[L]$	0 mM	Extracellular concentration of lactate	[19]
$[Pyr]$	0.12 mM	Intracellular concentration of pyruvate	[19]
ATP_{target}	2.8 mM	Intracellular concentration of ATP	[3]
U_G^{max}	1×10^{-7} mol/cell/s	Physiological uptake limit of glucose.	Estimated ¹
U_L^{max}	1×10^{-6} mol/cell/s	Physiological uptake limit of lactate.	Estimated
K_G	0.04 mM	Henri-Michaelis-Menten constant for glucose consumption	[15]
K_{O_2}	4.6×10^{-3} mM	Henri-Michaelis-Menten constant for oxygen consumption	[15]
K_L	21.78 mM	Henri-Michaelis-Menten constant for reverse LDH reaction	[37]
K_{pH}	6.9	pH at which the uptake of lactate is at half its maximum capacity.	Fitted from [19]
$p_{O_2}^G$	0.24	Constant of glucose uptake variation according to oxygen level	Fitted from [15]
$p_{O_2}^{ATP}$	1/cell/s	Constant that defines the rate of adaptation to missing ATP	Estimated
p_{Lac}^{Pyr}	1/cell/s	Constant that defines the rate of adaptation to missing Pyruvate	Estimated
$p_G^{pH_{max}}$	1.3	Maximum expression of glucose uptake when the pH is optimal.	Fitted from [19, 34]
pH_{max}	7.5	pH at which glucose uptake is maximal.	Fitted from [19, 34]
σ	0.27	Constant for spread in gaussian term of the glucose uptake	Fitted from [19, 34]
n	67.95	Hill coefficient for uptake of lactate according to pH.	Fitted from [19]
ATP_{demand}	[0.1; 0.2495; 1] $\times 10^{-5}$ mol/cell/s	ATP needs for a cell from low to high removed from the pool at each time step	Estimated ²

algorithm adapted to the stiffness of the problem (more details are available on the module documentation page): https://diffreq.sciml.ai/stable/solvers/ode_solve/.

The julia code is available in jupyter notebook format (.ipynb) at the following link: https://github.com/pierrejacquet/ATP_metabolism_Julia

2.3.2 Cell population level

To produce the spheroid simulation, we have integrated our model of cell energy metabolism as a module in PhysiCell (v1.5.2 available at <http://physicell.org/>) [39], an open source physics-based cell simulator that manages, among other things, the diffusion of substrates in the culture medium and provides tools to define cell cycle, division rates, necrotic and apoptotic events. As an agent-based model, each cell is independent and has its own internal processes (cell cycle, energy metabolism). They interact with each other and share local resources. In our model implementation, the diffusive resources are: oxygen, glucose, lactate and protons. We have integrated each phase of the cell cycle. The standard duration of the cell cycle is fixed at 24 hours (G1: 11h, S: 8h, G2: 4h, M: 1h) [40], in a medium with optimal oxygenation (fixed at $pO_2 = 38$ mmHg, or 0.05282 mM). If oxygen is lacking, the duration of the G1 phase extends proportionally to the ratio: $pO_2/38$.

3 Results

3.1 Metabolic landscape depending on substrates availability

The model satisfies the experimental observations. To test the model the extracellular concentrations were taken between 0 and 0.1 mM for oxygen and between 0 and 5 mM for glucose. These values are compatible with *in vivo* concentrations. Consumption terms have been normalized to facilitate the comparison between conditions. As oxygen becomes scarce or the concentration of extracellular glucose increases, glucose uptake increases (Fig. 2A). Conversely, the presence of glucose lowers oxygen consumption (Fig. 2C). The effect of intracellular pH makes glucose consumption close to zero under acidic conditions (Fig. 2B). Consequently, oxygen uptake no longer depends on the presence or absence of glucose in the medium at acidic pH (Fig. 2D).

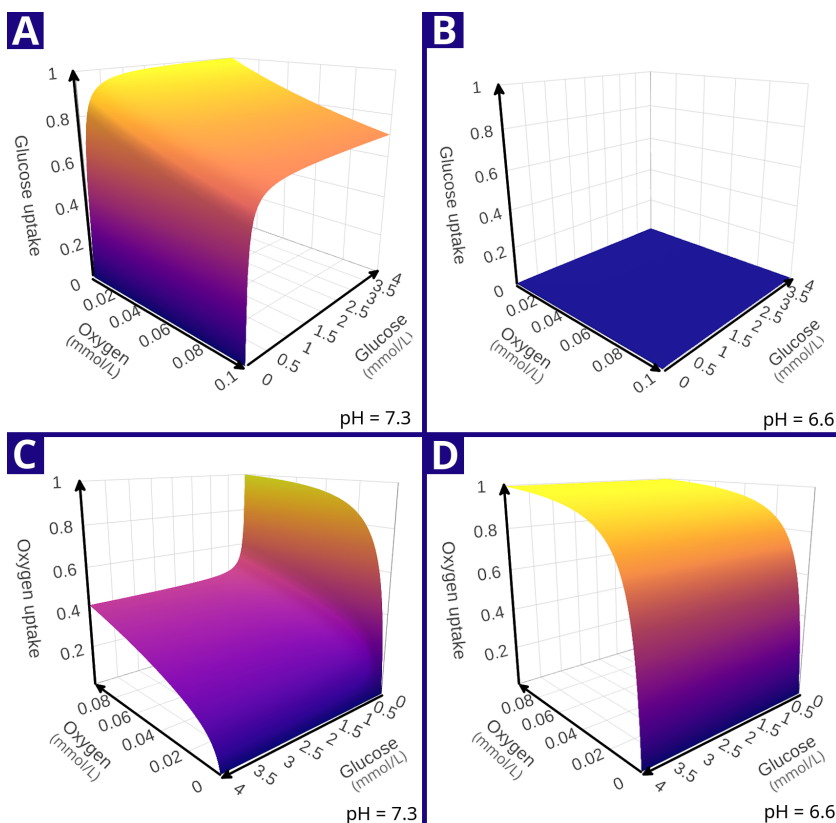


Figure 2: Normalized uptakes at different pH and extracellular concentrations of oxygen and glucose in *mM*. (A) Glucose uptake at pH 7.3. (B) Glucose uptake at pH 6.6. (C) Oxygen uptake at pH 7.3. (D) Oxygen uptake at pH 6.6.

From the previous uptakes, the ATP production rate can be calculated (see eq.8). Several models do not take into account the need for ATP as a mechanism for regulating the uptakes of the main substrates. However, it would be expensive for a cell to produce more ATP than it needs [41] (and regulatory mechanisms prevent this from happening), as well as it would be disadvantageous to under-produce ATP when surrounding resources are available. The result is that the cell cannot ensure a constant level of ATP as soon as the concentration of one of the extracellular substrates is changed. A specific level of ATP is required for the cell functioning and different energy mechanisms are involved to meet this level. Here, OXPHOS and

glycolysis cooperate to meet the ATP needs. Figure 3A shows that the cell - when the conditions are not extreme (glucose or oxygen concentrations not close to zero) - can plateau and stabilize its ATP production to respond to a fixed need. When the substrates are close to zero, ATP production decreases rapidly. Under acidic conditions (Fig. 3B), the cell loses its dependence on glucose. The production of ATP depends mainly on the concentration of oxygen (and of pyruvate not shown on this figure).

Figure 3C is a two-dimensional (2D) projection of figures 3A and 3B, with a logarithmic scale. This 2D representation is interesting for observing the levels of ATP production. Although it is not possible to reduce the cell state exclusively to its ability to maintain a certain level of ATP, it is clear that a proliferative cell uses more ATP than a quiescent cell [42]. It is then possible to associate different types of cells with different regions since the probability of encountering proliferative cells is greater in regions with high ATP production and necrotic cells in those with low ATP production.

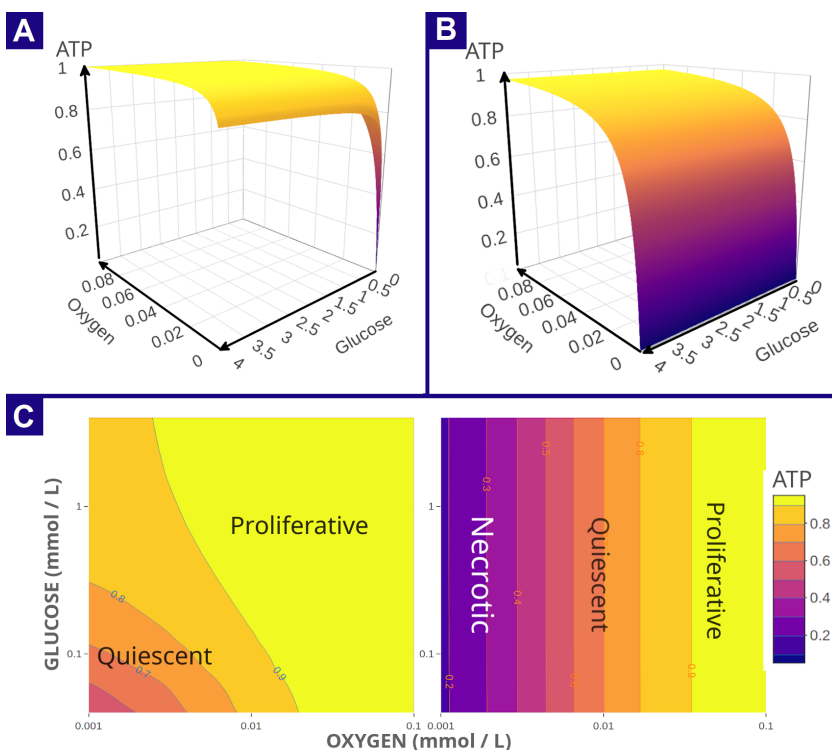


Figure 3: Normalized ATP production rate in multiple conditions. (A) ATP Production rate at pH 7.3. (B) ATP Production rate at pH 6.6. (C) Heatmap of ATP production rate at pH 7.3 (left) and 6.6 (right) with a logarithmic scale. For each ATP level a cellular state can be associated. Typically low levels of ATP correspond to quiescent cells (reduced metabolism) whereas high levels of ATP are associated to proliferating cells. The cell states are only mentioned here for illustrative purposes.

3.2 Adaptation dynamics of the cell metabolism

Cellular energy metabolism is often reduced to one observation at a given point in time, however it is a highly dynamic process. The cell constantly adapts to the changing environment and to its energy needs (mass production, division, *etc*). It therefore makes sense to consider the temporal evolution of the system given the environmental context. Here we consider three typical situations corresponding to idealized cases

in order to explore the model behavior:

1. a case where oxygen is non-limiting which is compatible with 2D cell cultures (*in vitro*);
2. a case where oxygen is limiting which is compatible with a poorly perfused environment;
3. a case where oxygen varies that mimics tumor angiogenesis.

For each of these three different environmental conditions, we consider three different levels of cell energy demand: low, medium and high.

Figure 4 presents the *non-limiting oxygen case*, where oxygen is maintained at a constant level throughout the simulation. Glucose is, on the other hand, consumed over time and decreases with an intensity linked to cellular energy demand. We note that for higher energy demands, glucose uptake saturates. Therefore, the drop in glucose concentration is the same for medium and high ATP demands (both are beyond the saturation level). For low energy demand, OXPHOS is low, because there is no need for more ATP. This low OXPHOS is insufficient to absorb all the pyruvate produced by glycolysis. As a result, the excess pyruvate is converted into lactate, which is excreted thus increasing the acidity. This drop in pH creates a negative feedback on glucose uptake until equilibrium is reached between glycolytic flux and OXPHOS. In other words the production of pyruvate (by glycolysis) and the consumption (by OXPHOS) become equal thus stabilizing the pH. This corresponds to a glycolytic contribution to ATP production of 5.5%.

When the demand for ATP is high, the glycolysis is not sufficient to produce the pyruvate which feeds the OXPHOS flux for which the oxygen uptake is high. As a consequence, pyruvate drops to extinction. Since the OXPHOS cannot be fueled, the high level of ATP cannot be maintained and drops too. We note that this situation depicts an extreme case proposed as an illustrative example, which is rarely observed *in vivo* because cell metabolism is drastically reduced in those extreme conditions. Moreover, there are numerous alternative energy substrates and pathways that can be used to produce energy and that we have not considered here.

Figure 5 shows the *limiting oxygen case*, where oxygen is rapidly consumed over time. There are three oxygen drop intensities which are related to the three levels of ATP demand. For the low ATP demand, we initially observe the same dynamics as in the previous case: the production of pyruvate (by glycolysis) is greater than the consumption of pyruvate (via OXPHOS). The surplus of pyruvate is converted into lactate and comes out of the cell with a proton until the pH stabilizes, indicating the equilibrium between OXPHOS and glycolysis. As soon as anoxia is reached, OXPHOS stops and the pyruvate is entirely converted into lactate. Lactate is excreted and this leads to a second acidic drop.

For the high ATP demand, there is a strong decrease in pyruvate since OXPHOS consumes more pyruvate than glycolysis can produce. As soon as the oxygen disappears, OXPHOS stops and the pyruvate pool fills up. During the initial decrease in oxygen, glucose uptake transiently increases to saturation (limited uptake capacity). This dramatically increases the acidity which ultimately leads to the collapse of glucose uptake.

Figure 6 presents a case with *varying oxygen conditions* which can be considered as a representation of the effects of tumor angiogenesis. It is well known that the angiogenic network is very unstable leading to oscillating oxygen conditions with a wide range of periodicities ranging from seconds to several hours [43]. We have chosen here to simulate the oxygen cycle with a periodicity of 20 hours. This periodicity was chosen to enhance the observed effects and increase the contrast with the previous case.

For the high ATP demand, we again observe the same dynamics as in the previous cases. Pyruvate is completely depleted in OXPHOS. At first, the amount of pyruvate remains sufficient in the cell, despite its

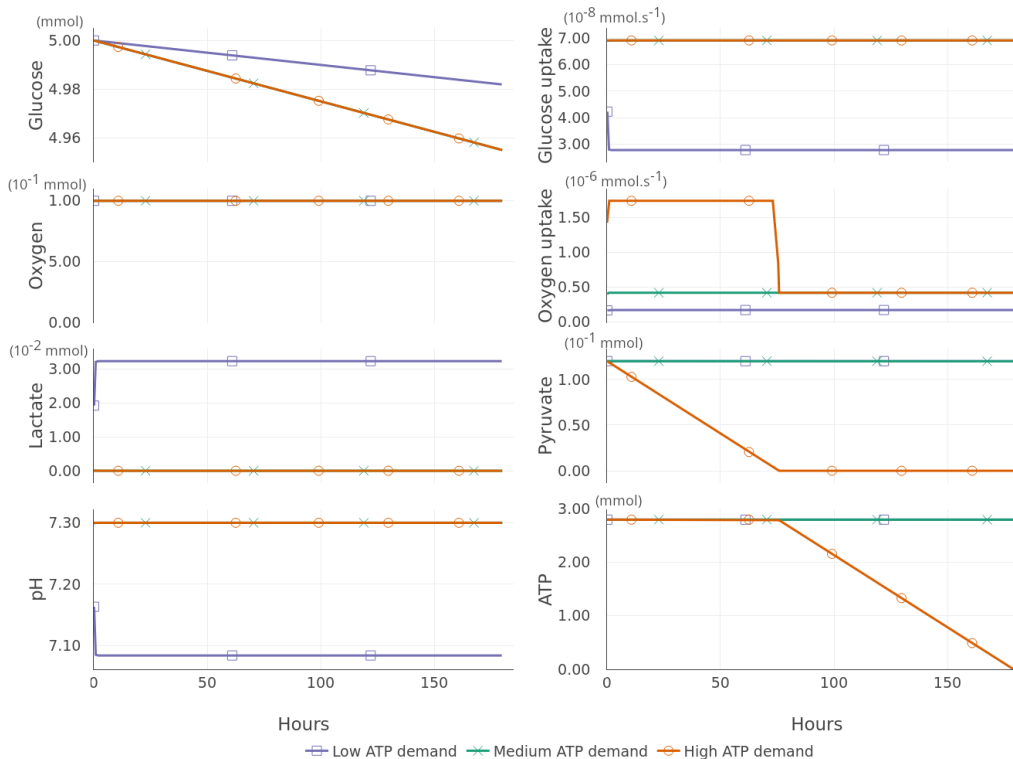


Figure 4: Evolution of the main metabolic molecules and uptake rates of glucose and oxygen as a function of the cell energy demand from low to high. Oxygen is non-limiting.

decrease, until it drops down. Small amounts are cyclically restored by glycolysis and are instantly consumed as soon as the oxygen level allows.

When the energy load is lower, sustained oscillations of lactate and pH are observed, caused by the periodic shutdown of OXPHOS. The frequency of oxygen oscillations is fast enough to maintain an almost constant level of pyruvate restored by lactate. We note that we did not take into account the time required to convert lactate to pyruvate - in our model it is considered an instantaneous process - this leads to sharp pH oscillations which are not observed experimentally. However our goal at this point is to highlight the possible emerging metabolic behaviors rather than being quantitatively realistic.

These results clearly show that - depending on the oxygen constraint - glycolysis and OXPHOS cooperate to sustain, as far as possible, the energy demand in terms of ATP production. This cooperation is mediated by the amount of pyruvate which is - within the framework of our model approximation - the product of the first and source of the second. This contradicts a *switch mechanism* of the metabolism which implies an alternate and exclusive (*i.e.* dual) functioning of the two metabolic modes.

3.3 Metabolism at the cell population level

The spatial dimension is often overlooked in most studies of cell metabolism, including theoretical and experimental approaches. In the first case, most models focus on the mechanisms on individual cells (as we have done so far) and in the second experimental case, most of the measurements are made at the level of the entire

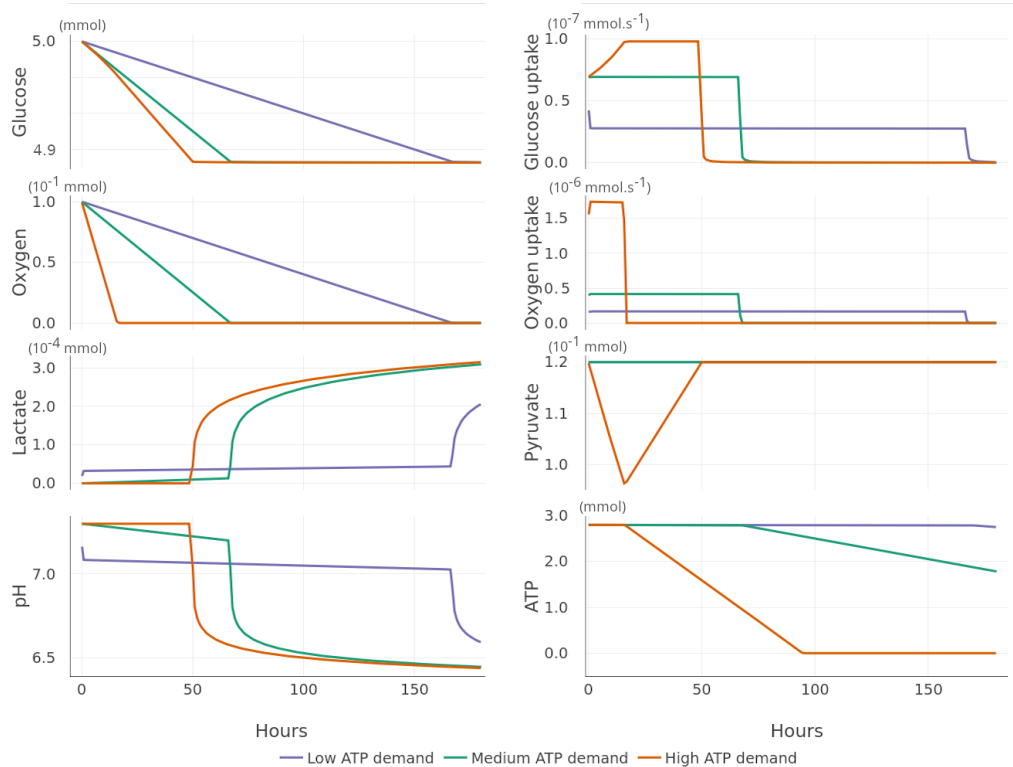


Figure 5: Evolution of the main metabolic molecules and uptake rates of glucose and oxygen as a function of the cell energy demand from low to high. Oxygen is limiting.

cell populations, either on two dimensional cell cultures or on three dimensional spheroids. Extracellular Flux Analysers (Seahorse) [44] are widely used to characterize cell metabolisms based on measurements of OCR (Oxygen Consumption Rate) and ECAR (Extracellular Acidification Rate). However, these measurements reflect the average values for the entire cell population, when in fact a high discrepancy exists between cells depending on the local environmental context and cell state [45, 46]. While the use of this device makes more sense for two dimensional cell cultures, where the environment is assumed to be homogeneous, it is clearly not suitable for spheroids where the inner cells do not have the same access to resources compared to the peripheral cells.

In this section, we aim to specifically highlight the heterogeneity that exists in a spheroid due to the gradients of the main substrates from the periphery to the core (Fig. 7, upper graph). These gradients are mainly due to the increase in the density of cells in the center which consume more nutrients and impede their diffusion. As a result, resource gradients (oxygen and glucose) induce the emergence of different metabolic states depending on cell depth in the spheroid. For the simulation shown in figure 7, the initial radius of the cell is $8.41\mu\text{m}$, the cell density is $9 \times 10^4 \text{ cells}/\mu\text{l}$ and the diameter of the spheroid is $800 \mu\text{m}$ at the end of the simulation. The simulation is performed on a cubic domain $1020 \mu\text{m}$ wide. The initial state corresponds to a tumor spheroid immersed in a highly hypoxic environment. To highlight the different metabolic states that can be encountered, we did not consider the cell states transitions from proliferation to necrosis. However we took into account the increase in cell cycle duration induced by the lack of oxygen and mediated by HIF-1 α [47].

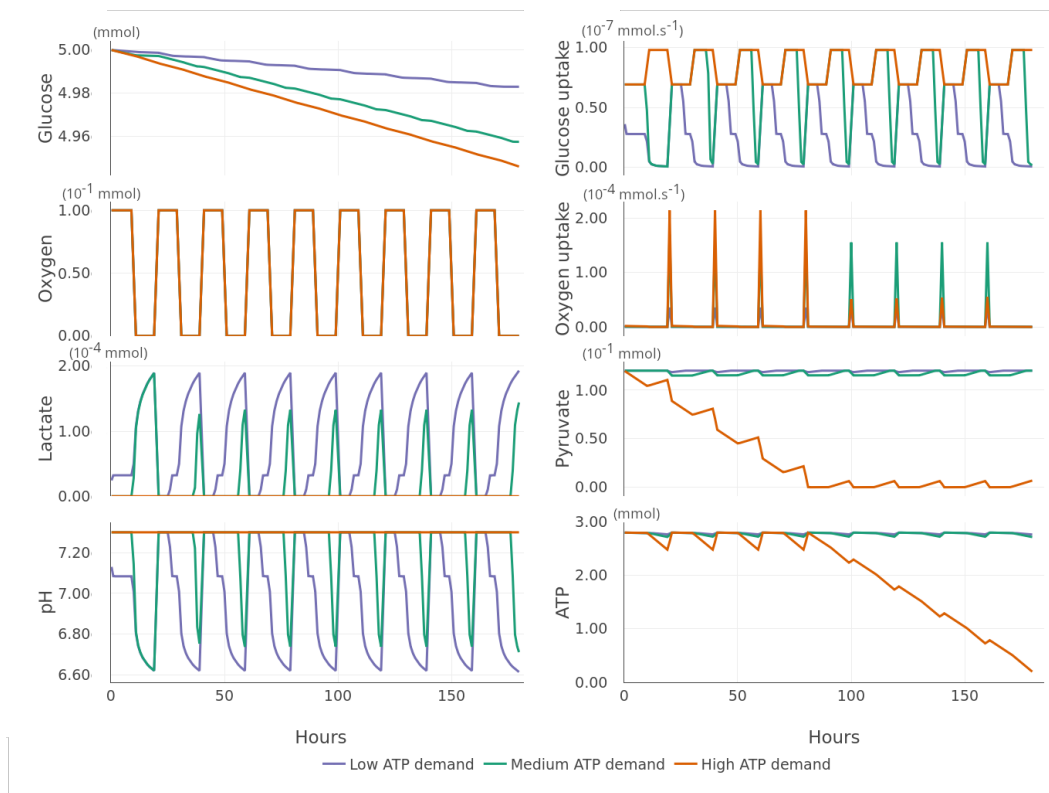


Figure 6: Evolution of the main metabolic molecules and uptake rates of glucose and oxygen as a function of the cell energy demand from low to high. Oxygen is varying.

Figure 7A clearly shows that the contribution of glycolysis is much higher at the center where the oxygen level is low (Fig. 7, upper graph). Consequently, the pH is lower in the center and is directly correlated with the glucose uptake gradient (Fig. 7D and 7B). On the other hand, the oxygen uptake gradient is steeper from the center to the periphery because the oxygen consumption is higher than glucose and its initial concentration is lower which makes it more sensitive to depletion (Fig. 7C). The net secretion of lactate presents an interesting profile (Fig. 7E) with a middle layer of lower secretion. This is explained by a high OXPHOS activity requiring pyruvate at the level of the outer layer. This leads to a lower level of secreted lactate as glycolysis is slightly diminished from the periphery. At the other end, in the center, OXPHOS is greatly reduced because the oxygen level is low. This reduces the need for pyruvate (by OXPHOS), so excess pyruvate is converted to lactate. The net secretion of lactate thus reaches almost the same level at the heart of the spheroid than at its periphery. Finally, ATP is globally maintained around its basal level, except in the center where oxygen is low and OXPHOS is reduced (Fig. 7F). We note that glycolysis is not able to maintain the level of ATP. This would typically induce a transition to a reduced metabolism such as quiescence. However, the cell usually reduces its energy needs long before it runs out of ATP, because HIF triggers the entry into quiescence as the oxygen level is too low.

Figure 7E, which shows net lactate production, exhibits a non-homogeneous Warburg effect. Its intensity - defined by the importance of the contribution of glycolysis (Fig. 7A) - depends on the gradient stiffness of the substrates. Moreover, we observe here one instant of an evolving process which corresponds to a transient

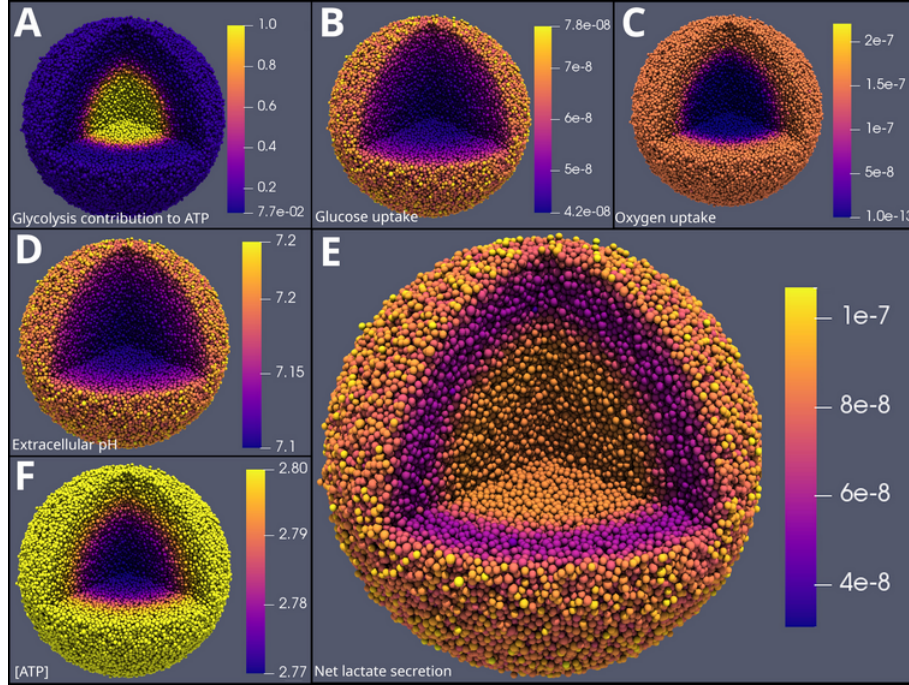
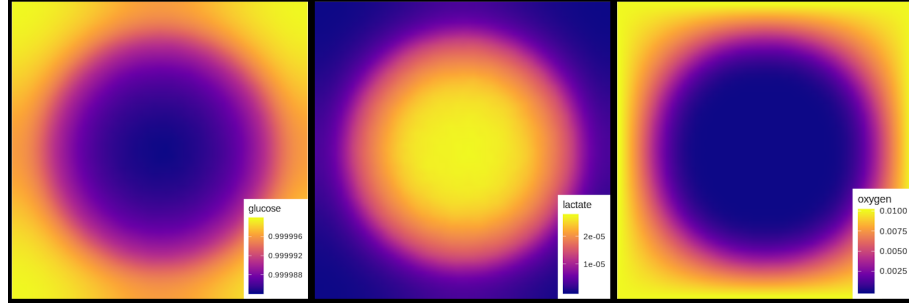


Figure 7: Upper graph: distribution of molecules and acidity in the medium of the spheroid simulation. From left to right: Glucose concentration in mM (initial concentration in the medium: 1mM); Lactate concentration in mM (initial concentration in the medium: 0mM); Oxygen concentration in mM. The oxygen concentration is fixed (0.01 mM) at the boundary of the simulation domain. Spheroid simulation at 10 days using Physicell[39]. Initial medium concentrations: 2mM glucose, 0.01mM oxygen, pH=7.3, no lactate. Each figure represents the same spheroid with coloration for different parameters. **A.** Glycolysis contribution to ATP production; **B.** Glucose uptake in $mM.s^{-1}$; **C.** Oxygen uptake in $mM.s^{-1}$; **D.** Extracellular pH; **E.** Net lactate secretion in $mM.s^{-1}$; **F.** ATP level in mM.

state. This shows that this effect is not a well-defined state with a switch-like dynamic but a progressive event. We note that our simulation is only one possible configuration given our choice of parameters. Other cases could be generated. For example, a sharper pH gradient from center to the periphery leading to extinction of glycolysis would have led to different scenarios of cell metabolism.

4 Discussion

The model of cell energy metabolism that we proposed in this study integrates the most recent knowledge. It is based on a number of key experimental observations and established facts. It is moreover adjusted and parameterized on the basis of experimental data. The model focuses on the glycolysis-OXPHOS relationship and in particular emphasizes the role of lactate as a substrate, as well as the central role of pyruvate in the regulation of metabolism. The latter makes the link between glycolysis, fermentation and OXPHOS (after conversion in the TCA cycle).

The oxidation of pyruvate requires that it be imported into the mitochondrial matrix and subjected to the activity of the pyruvate dehydrogenase (PDH) complex. The activity of this enzyme is regulated by several conditions, such as CoA levels, NAD^+/NADH ratio. It is a relatively long process compared to fermentation. Glycolysis is less efficient than OXPHOS [1, 8, 48, 49] in terms of ATP produced per glucose molecule. However, in terms of ATP molecules produced by unit of time, glycolysis is a much faster process (about a hundred times faster [50]). It allows the cell to adapt quickly in order to meet immediate energy needs. Glycolysis is not efficient for the amount of glucose consumed but may be a better alternative than OXPHOS to produce energy very quickly to meet acute needs [27, 51]. When the glycolytic flux exceeds the maximum activity of PDH, the pyruvate excess is spontaneously converted into lactate [48].

It is also interesting to note that while glucose consumption and lactate production decrease with pH, the concentration of intracellular lactate increases. This mechanism suggests that the cell recovers extracellular lactate to maintain its pyruvate level at a constant value. Indeed, under conditions of lactic acidosis, the protons level being higher outside the cell, the entry of lactate via the MCT1 transporter, is facilitated [19]. One could imagine this system as a hydraulic dam. The dam retain the pyruvates upstream, which finds its source in glycolysis. Depending on the energy needs, the dam is opened with more or less intensity (OXPHOS). Sometimes the level overflows, the dam then lets the surplus pass without producing energy. Pyruvate is then transformed into lactate. Conversely, when pyruvate is lacking, the dam is supplied by the source of lactate. The simulations that we carried out to observe how the imposed environmental constraints (*i.e.* the oxygen level and acidity) and the imposed energy needs push the cell to adapt, highlight this dam mechanism. Our results clearly show that glycolysis and OXPHOS are used concomitantly and cooperatively [21], with a gradation in their relative contributions to ATP production that depends on available resources and pH.

These results contrast somehow with the current view of tumor cell metabolism, which is portrayed as abnormal and characterized by increased glycolysis even in the presence of oxygen, the so-called Warburg effect. It seems important to us to stick to the original definition of the Warburg effect, which does not presuppose the presence of oxygen [5, 6, 51]. This effect - *i.e.* the overproduction of lactate - is recognized as a hallmark of cancer. However, recent experiments have shown that by acidifying its environment the tumor cell progressively self-inhibits this phenotype [19]. By integrating this observation into our model, our simulations show that the Warburg effect is indeed only transient (limited in time) and contextual (dependent on acidity). The increase in glycolytic activity in the presence of oxygen is not a specific phenomenon of cancer. There are brain regions that primarily use aerobic glycolysis [52], as well as endothelial cells during angiogenesis [53], and mesenchymal stem cells which primarily depend on glycolysis and require less oxygen [54]. It might be useful to recall that, from an evolutionary point of view, OXPHOS is a process that appeared after glycolysis. Primitive eukaryotic cells only became able to use oxygen after the endosymbiosis of proteobacteria. The eukaryotic cells have thus obtained by this mean an additional source of ATP pro-

duction, complementary to glycolysis, and which has been preserved until now.

Temporality, and more particularly the time scale with which changes in metabolism develop, has been neglected despite its importance. On a short time scale, our results contribute to show that the early tumor cell is able to gradually adapt its metabolism and the metabolic changes are reversible [27]. On a longer time scale, the metabolic evolution most likely depends on the history of stress (frequency and intensity of hypoxic events) that the cell has undergone. It is well known that HIF-1 α stabilization with hypoxia is a powerful driver of genetic instability [55].

The strength of our approach – based on a reduced model of cell metabolism – is that we have been able to show how some forms of metabolic cooperation between the two metabolic modes, glycolysis and OXPHOS, can already emerge from a limited number of molecular actors. This highlights the robustness of the biological system that can preserve its functions through alternative use of the available substrates. The limitation is that, other major molecular actors (such as NADH) and other key mechanisms (amino acid or fatty acid metabolisms, etc.) have not been considered. However our reduced model and its results provide a plausible experience of thought to test some potential scenarios and their validity. In our case, the results obtained provide enough arguments about the emerging metabolic adaptation to question the nature of the cancer metabolic phenotype itself. Further studies will be required to clarify this cancer metabolic status, but at least our reduced model proposes that – given the strong metabolic adaptability of the cell – it could be not much more different than that of a normal cell [56].

5 Conclusions

We have proposed a reduced model of cellular energy metabolism to demonstrate certain aspects of the glycolysis-OXPHOS relationship, in particular in the deregulated tumor microenvironment characterized by low oxygenation and a high level of acidity. The model was developed to manage the complexity of the different reactions and make sense of these reactions in space and time. The model, based on a few key experimental observations and well-established facts, emphasizes the role of lactate as a substrate. We first showed the central role of pyruvate in the regulation of metabolism. Our simulations also showed how imposed environmental constraints lead to metabolic adaptation to meet the increased energy demand. The results show the cooperation of the two metabolic modes which are not mutually exclusive. Our results thus tend to show that the Warburg effect is not necessarily an inherent characteristic of the tumor cell, but a spontaneous and transient adaptation mechanism to a disturbed environment. The notion of metabolic reprogramming associated with the Warburg effect is moreover questioned by several authors [57], emphasizing the fact that the adaptation of cellular metabolism is multifactorial and occurs at different levels beyond genetics and epigenetics. This could have implications for how therapies are viewed. The search for normalization of tumor acidity, for example, could become a good strategy.

Acknowledgements

This work is related to the POET project financed by INSERM/CNRS "Santé Numérique - 2019" (Grant Reference: 216669). We thank the Research Group GDR ImaBio (<http://imabio-cnrs.fr>) for partial funding of P.J.'s work. We also wish to warmly thank Paul Macklin for his help and support with PhysiCell that we used to make the spheroid simulation.

References

- [1] S. Devic, Warburg effect - a consequence or the cause of carcinogenesis?, *Journal of Cancer* 7 (7) (2016) 817–822. doi:10.7150/jca.14274.
- [2] P. J. Bhat, L. Darunte, V. Kareenhalli, J. Dandekar, A. Kumar, Can metabolic plasticity be a cause for cancer? Warburg–Waddington legacy revisited, *Clinical Epigenetics* 2 (2) (2011) 113–122. doi:10.1007/s13148-011-0030-x.
URL <http://www.clinicalepigeneticsjournal.com/content/2/2/>
- [3] J. H. van Beek, The dynamic side of the Warburg effect: glycolytic intermediate storage as buffer for fluctuating glucose and O₂ supply in tumor cells, *F1000Research* 7 (0) (2018) 1177. doi:10.12688/f1000research.15635.2.
- [4] O. Warburg, On the Origin of Cancer Cells, *Science* 123 (3191) (1956) 309–314. doi:10.1126/science.123.3191.309.
URL <http://www.sciencemag.org/cgi/doi/10.1126/science.123.3191.309>
- [5] S. A. Mookerjee, A. A. Gerencser, D. G. Nicholls, M. D. Brand, Quantifying intracellular rates of glycolytic and oxidative ATP production and consumption using extracellular flux measurements, *Journal of Biological Chemistry* 292 (17) (2017) 7189–7207. doi:10.1074/jbc.M116.774471.
- [6] A. Vazquez, J. Liu, Y. Zhou, Z. N. Oltvai, Catabolic efficiency of aerobic glycolysis: The Warburg effect revisited, *BMC Systems Biology* 4 (1) (2010) 58. doi:10.1186/1752-0509-4-58.
URL <https://bmcsystbiol.biomedcentral.com/articles/10.1186/1752-0509-4-58>
- [7] M. V. Liberti, J. W. Locasale, C. C. Biology, C. C. Biology, The Warburg Effect: How Does it Benefit Cancer Cells?, *Trends in Biochemical Sciences* 41 (3) (2016) 211–218. doi:10.1016/j.tibs.2015.12.001.
URL <http://www.ncbi.nlm.nih.gov/pubmed/26778478><http://www.pubmedcentral.nih.gov/articlerender.fcgi?artid=PMC4783224><https://linkinghub.elsevier.com/retrieve/pii/S0968000415002418><http://linkinghub.elsevier.com/retrieve/pii/S0968000415002418>
0Apapers3://publi
- [8] R. A. Gatenby, R. J. Gillies, Why do cancers have high aerobic glycolysis?, *Nature Reviews Cancer* 4 (11) (2004) 891–899. doi:10.1038/nrc1478.
- [9] R. J. Gillies, I. Robey, R. A. Gatenby, Causes and Consequences of Increased Glucose Metabolism of Cancers, *Journal of Nuclear Medicine* 49 (Suppl_2) (2008) 24S–42S. doi:10.2967/jnumed.107.047258.
URL <http://jnm.snmjournals.org/cgi/doi/10.2967/jnumed.107.047258>
- [10] C. Nazaret, J. P. Mazat, An old paper revisited: "A mathematical model of carbohydrate energy metabolism. Interaction between glycolysis, the Krebs cycle and the H-transporting shuttles at varying ATPases load" by V.V. Dynnik, R. Heinrich and E.E. Sel'kov, *Journal of Theoretical Biology* 252 (3) (2008) 520–529. doi:10.1016/j.jtbi.2008.01.003.
- [11] C. Phipps, H. Molavian, M. Kohandel, A microscale mathematical model for metabolic symbiosis: Investigating the effects of metabolic inhibition on ATP turnover in tumors, *Journal of Theoretical Biology* 366 (2015) 103–114. doi:10.1016/j.jtbi.2014.11.016.
URL <http://dx.doi.org/10.1016/j.jtbi.2014.11.016>

- [12] M. B. Kuznetsov, A. V. Kolobov, Transient alleviation of tumor hypoxia during first days of antiangiogenic therapy as a result of therapy-induced alterations in nutrient supply and tumor metabolism – Analysis by mathematical modeling, *Journal of Theoretical Biology* 451 (2018) 86–100. doi:10.1016/j.jtbi.2018.04.035.
URL <https://doi.org/10.1016/j.jtbi.2018.04.035>
- [13] R. Venkatasubramanian, M. A. Henson, N. S. Forbes, Incorporating energy metabolism into a growth model of multicellular tumor spheroids, *Journal of Theoretical Biology* 242 (2) (2006) 440–453. doi:10.1016/j.jtbi.2006.03.011.
- [14] M. Shan, D. Dai, A. Vudem, J. D. Varner, A. D. Stroock, Multi-scale computational study of the Warburg effect, reverse Warburg effect and glutamine addiction in solid tumors, *PLoS Computational Biology* 14 (12) (2018) e1006584. doi:10.1371/journal.pcbi.1006584.
URL <http://dx.plos.org/10.1371/journal.pcbi.1006584>
- [15] J. J. Casciari, S. V. Sotirchos, R. M. Sutherland, Variations in tumor cell growth rates and metabolism with oxygen concentration, glucose concentration, and extracellular pH, *Journal of Cellular Physiology* 151 (2) (1992) 386–394. doi:10.1002/jcp.1041510220.
URL <http://doi.wiley.com/10.1002/jcp.1041510220>
- [16] J. J. Casciari, S. V. Sotirchos, R. M. Sutherland, Mathematical modelling of microenvironment and growth in emt6/ro multicellular tumour spheroids, *Cell Proliferation* 25 (1) (1992) 1–22. arXiv:<https://onlinelibrary.wiley.com/doi/pdf/10.1111/j.1365-2184.1992.tb01433.x>, doi:<https://doi.org/10.1111/j.1365-2184.1992.tb01433.x>.
URL <https://onlinelibrary.wiley.com/doi/abs/10.1111/j.1365-2184.1992.tb01433.x>
- [17] N. Jagiella, B. Müller, M. Müller, I. E. Vignon-Clementel, D. Drasdo, Inferring Growth Control Mechanisms in Growing Multi-cellular Spheroids of NSCLC Cells from Spatial-Temporal Image Data, *PLoS Computational Biology* 12 (2) (2016) e1004412. doi:10.1371/journal.pcbi.1004412.
URL <https://dx.plos.org/10.1371/journal.pcbi.1004412>
- [18] C. DuBois, J. Farnham, E. Aaron, A. Radunskaya, A multiple time-scale computational model of a tumor and its micro environment, *Mathematical Biosciences and Engineering* 10 (1) (2012) 121–150. doi:10.3934/mbe.2013.10.121.
- [19] J. Xie, H. Wu, C. Dai, Q. Pan, Z. Ding, D. Hu, B. Ji, Y. Luo, X. Hu, Beyond Warburg effect - Dual metabolic nature of cancer cells, *Scientific Reports* 4 (2014) 1–12. doi:10.1038/srep04927.
- [20] X. Hu, M. Chao, H. Wu, Central role of lactate and proton in cancer cell resistance to glucose deprivation and its clinical translation, *Signal Transduction and Targeted Therapy* 2 (December 2016) (2017) 16047. doi:10.1038/sigtrans.2016.47.
URL <http://dx.doi.org/10.1038/sigtrans.2016.47>
- [21] J. Zheng, Energy metabolism of cancer: Glycolysis versus oxidative phosphorylation (review), *Oncology Letters* 4 (6) (2012) 1151–1157. doi:10.3892/ol.2012.928.
URL <https://www.spandidos-publications.com/10.3892/ol.2012.928>
- [22] P. Rich, The molecular machinery of Keilin’s respiratory chain, *Biochemical Society Transactions* 31 (6) (2003) 1095–1105. doi:10.1042/bst0311095.
URL <http://www.biochemsoctrans.org/cgi/doi/10.1042/bst0311095>

- [23] P. C. Hinkle, P/O ratios of mitochondrial oxidative phosphorylation, *Biochimica et Biophysica Acta (BBA) - Bioenergetics* 1706 (1-2) (2005) 1–11. doi:10.1016/j.bbabi.2004.09.004.
URL <https://linkinghub.elsevier.com/retrieve/pii/S0005272804002701>
- [24] K. Ashizawa, M. C. Willingham, C. M. Liang, S. Y. Cheng, In vivo regulation of monomer-tetramer conversion of pyruvate kinase subtype M2 by glucose is mediated via fructose 1,6-bisphosphate, *Journal of Biological Chemistry* 266 (25) (1991) 16842–16846.
- [25] S. Mazurek, C. B. Boschek, F. Hugo, E. Eigenbrodt, Pyruvate kinase type M2 and its role in tumor growth and spreading, *Seminars in Cancer Biology* 15 (4) (2005) 300–308. doi:10.1016/j.semcancer.2005.04.009.
URL <https://linkinghub.elsevier.com/retrieve/pii/S1044579X0500026X>
- [26] W. Mueller-Klieser, J. P. Freyer, R. M. Sutherland, Influence of glucose and oxygen supply conditions on the oxygenation of multicellular spheroids, *British Journal of Cancer* 53 (3) (1986) 345–353. doi:10.1038/bjc.1986.58.
- [27] H. Wu, M. Ying, X. Hu, Lactic acidosis switches cancer cells from aerobic glycolysis back to dominant oxidative phosphorylation, *Oncotarget* 7 (26) (2016) 36–38. doi:10.18632/oncotarget.9746.
- [28] S. Fulda, K.-M. M. Debatin, HIF-1-regulated glucose metabolism: A key to apoptosis resistance?, *Cell Cycle* 6 (7) (2007) 790–792. doi:10.4161/cc.6.7.4084.
URL <http://www.tandfonline.com/doi/abs/10.4161/cc.6.7.4084>
- [29] K. Dietl, K. Renner, K. Dettmer, B. Timischl, K. Eberhart, C. Dorn, C. Hellerbrand, M. Kastenberger, L. A. Kunz-Schughart, P. J. Oefner, R. Andreesen, E. Gottfried, M. P. Kreutz, Lactic Acid and Acidification Inhibit TNF Secretion and Glycolysis of Human Monocytes, *The Journal of Immunology* 184 (3) (2010) 1200–1209. doi:10.4049/jimmunol.0902584.
URL <http://www.jimmunol.org/lookup/doi/10.4049/jimmunol.0902584>
- [30] M. P. Fellenz, L. E. Gerweck, Influence of Extracellular pH on Intracellular pH and Cell Energy Status: Relationship to Hyperthermic Sensitivity, *Radiation Research* 116 (2) (1988) 305. doi:10.2307/3577466.
URL <https://www.jstor.org/stable/3577466?origin=crossref>
- [31] I. F. Robey, A. D. Lien, S. J. Welsh, B. K. Baggett, R. J. Gillies, Hypoxia-Inducible Factor-1 α and the Glycolytic Phenotype in Tumors, *Neoplasia* 7 (4) (2005) 324–330. doi:10.1593/neo.04430.
URL <https://linkinghub.elsevier.com/retrieve/pii/S1476558605800636>
- [32] R. Courtney, D. C. Ngo, N. Malik, K. Ververis, S. M. Tortorella, T. C. Karagiannis, Cancer metabolism and the Warburg effect: the role of HIF-1 and PI3K, *Molecular Biology Reports* 42 (4) (2015) 841–851. doi:10.1007/s11033-015-3858-x.
URL <http://link.springer.com/10.1007/s11033-015-3858-x>
- [33] H. Choudhry, A. L. Harris, Advances in Hypoxia-Inducible Factor Biology, *Cell Metabolism* 27 (2) (2018) 281–298. doi:10.1016/j.cmet.2017.10.005.
URL <https://linkinghub.elsevier.com/retrieve/pii/S1550413117306174>
- [34] M. L. Halperin, H. P. Connors, A. S. Relman, M. L. Karnovsky, Factors that control the effect of pH on glycolysis in leukocytes., *The Journal of biological chemistry* 244 (2) (1969) 384–90.
URL <http://www.ncbi.nlm.nih.gov/pubmed/4237582>

- [35] D. F. Wilson, Oxidative phosphorylation: regulation and role in cellular and tissue metabolism, *Journal of Physiology* 595 (23) (2017) 7023–7038. doi:10.1113/JP273839.
URL <http://doi.wiley.com/10.1113/JP273839>
- [36] N. Vijay, M. Morris, Role of Monocarboxylate Transporters in Drug Delivery to the Brain, *Current Pharmaceutical Design* 20 (10) (2014) 1487–1498. doi:10.2174/13816128113199990462.
URL <http://www.ncbi.nlm.nih.gov/pubmed/23789956><http://www.pubmedcentral.nih.gov/articlerender.fcgi?artid=PMC4084603><http://www.eurekaselect.com/openurl/content.php?genre=article&issn=1381-6128&volume=20&issue=10&spage=1487>
- [37] A. Talaiezhadeh, A. Shahriari, M. Tabandeh, P. Fathizadeh, S. Mansouri, Kinetic characterization of lactate dehydrogenase in normal and malignant human breast tissues, *Cancer Cell International* 15 (1) (2015) 19. doi:10.1186/s12935-015-0171-7.
URL <http://www.cancerci.com/content/15/1/19>
- [38] C. Rackauckas, Q. Nie, DifferentialEquations.jl – A Performant and Feature-Rich Ecosystem for Solving Differential Equations in Julia, *Journal of Open Research Software* 5. doi:10.5334/jors.151.
URL <http://openresearchsoftware.metajnl.com/articles/10.5334/jors.151/>
- [39] A. Ghaffarizadeh, R. Heiland, S. H. Friedman, S. M. Mumenthaler, P. Macklin, PhysiCell: An open source physics-based cell simulator for 3-D multicellular systems, *PLOS Computational Biology* 14 (2) (2018) e1005991. doi:10.1371/journal.pcbi.1005991.
URL <https://dx.plos.org/10.1371/journal.pcbi.1005991>
- [40] G. M. Cooper, R. E. Hausman, *The Cell: A Molecular Approach* 2nd Edition, 2007.
- [41] T. Epstein, R. A. Gatenby, J. S. Brown, The Warburg effect as an adaptation of cancer cells to rapid fluctuations in energy demand, *PLoS ONE* 12 (9) (2017) 1–14. doi:10.1371/journal.pone.0185085.
- [42] N. Yalamanchili, A. Kriete, D. Alfego, K. M. Danowski, C. Kari, U. Rodeck, Distinct Cell Stress Responses Induced by ATP Restriction in Quiescent Human Fibroblasts, *Frontiers in Genetics* 7 (OCT). doi:10.3389/fgene.2016.00171.
URL <http://journal.frontiersin.org/article/10.3389/fgene.2016.00171>
- [43] M. W. Dewhirst, Relationships between Cycling Hypoxia, HIF-1, Angiogenesis and Oxidative Stress, *Radiation Research* 172 (6) (2009) 653–665. doi:10.1667/RR1926.1.
URL <http://www.bioone.org/doi/10.1667/RR1926.1>
- [44] J. Zhang, Q. Zhang, Using Seahorse Machine to Measure OCR and ECAR in Cancer Cells, in: *Methods in Molecular Biology*, Vol. 1928, 2019, pp. 353–363. doi:10.1007/978-1-4939-9027-6_{_}18.
URL http://link.springer.com/10.1007/978-1-4939-9027-6_18
- [45] P. Danhier, P. Bański, V. L. Payen, D. Grasso, L. Ippolito, P. Sonveaux, P. E. Porporato, Cancer metabolism in space and time: Beyond the Warburg effect, *Biochimica et Biophysica Acta (BBA) - Bioenergetics* 1858 (8) (2017) 556–572. doi:10.1016/j.bbabi.2017.02.001.
URL <https://linkinghub.elsevier.com/retrieve/pii/S0005272817300233>
- [46] T. M. Heaster, B. A. Landman, M. C. Skala, Quantitative spatial analysis of metabolic heterogeneity across in vivo and in vitro tumor models, *Frontiers in Oncology* 9. doi:10.3389/fonc.2019.01144.

- [47] B. Bedessem, A. Stéphanou, A mathematical model of HiF-1 α -mediated response to hypoxia on the G1/S transition, *Mathematical Biosciences* 248 (1) (2014) 31–39. doi:10.1016/j.mbs.2013.11.007.
- [48] R. J. DeBerardinis, J. J. Lum, G. Hatzivassiliou, C. B. Thompson, The Biology of Cancer: Metabolic Reprogramming Fuels Cell Growth and Proliferation, *Cell Metabolism* 7 (1) (2008) 11–20. doi:10.1016/j.cmet.2007.10.002.
- [49] D. Hanahan, R. A. Weinberg, Hallmarks of cancer: The next generation, *Cell* 144 (5) (2011) 646–674. doi:10.1016/j.cell.2011.02.013.
URL <http://www.ncbi.nlm.nih.gov/pubmed/21376230>
- [50] S. Ganapathy-Kanniappan, J.-F. H. Geschwind, Tumor glycolysis as a target for cancer therapy: progress and prospects, *Molecular Cancer* 12 (1) (2013) 152. doi:10.1186/1476-4598-12-152.
- [51] X. L. Zu, M. Guppy, Cancer metabolism: Facts, fantasy, and fiction, *Biochemical and Biophysical Research Communications* 313 (3) (2004) 459–465. doi:10.1016/j.bbrc.2003.11.136.
- [52] S. N. Vaishnavi, A. G. Vlassenko, M. M. Rundle, A. Z. Snyder, M. A. Mintun, M. E. Raichle, Regional aerobic glycolysis in the human brain, *Proceedings of the National Academy of Sciences* 107 (41) (2010) 17757–17762. doi:10.1073/pnas.1010459107.
URL <http://www.pnas.org/lookup/doi/10.1073/pnas.1010459107>
- [53] G. Fitzgerald, I. Soro-Arnaiz, K. De Bock, The Warburg effect in endothelial cells and its potential as an anti-angiogenic target in cancer, *Frontiers in Cell and Developmental Biology* 6 (2018) 100. doi:10.3389/fcell.2018.00100.
- [54] J. M. Funes, M. Quintero, S. Henderson, D. Martinez, U. Qureshi, C. Westwood, M. O. Clements, D. Bourbouli, R. B. Pedley, S. Moncada, C. Boshoff, Transformation of human mesenchymal stem cells increases their dependency on oxidative phosphorylation for energy production, *Proceedings of the National Academy of Sciences* 104 (15) (2007) 6223–6228. doi:10.1073/pnas.0700690104.
URL <http://www.pnas.org/cgi/doi/10.1073/pnas.0700690104>
- [55] K. R. Luoto, R. Kumareswaran, R. G. Bristow, Tumor hypoxia as a driving force in genetic instability, *Genome Integrity* 4 (1) (2013) 5. doi:10.1186/2041-9414-4-5.
URL <http://genomeintegrity.biomedcentral.com/articles/10.1186/2041-9414-4-5>
- [56] P. Jacquet, A. Stéphanou, Searching for the metabolic signature of cancer: A review from warburg’s time to now, *Biomolecules* 12 (1412). doi:10.3390/biom12101412.
- [57] P. Jacquet, A. Stéphanou, Metabolic reprogramming, questioning, and implications for cancer., *Biology* 10 (129). doi:10.3390/biology10020129.